Journal of Advanced Ceramics
2013, 2(4): 313–317
DOI: 10.1007/s40145-013-0077-6

ISSN 2226-4108
CN 10-1154/TQ

Research Article

Corrosion behavior of Ti_3AlC_2 in molten KOH at 700 °C

Dandan SUN, Aiguo ZHOU*, Zhengyang LI, Libo WANG

Cultivating Base for Key Laboratory of Environment-friendly Inorganic Materials in University of Henan Province, School of Materials Science and Engineering, Henan Polytechnic University, Jiaozuo 454000, Henan, China

Received: April 07, 2013; Revised: July 23, 2013; Accepted: August 08, 2013

Abstract: This paper investigated the corrosion behaviors of Ti_3AlC_2 at 700 ℃ in molten KOH with various mass ratios. If the mass ratio of KOH:Ti_3AlC_2⩽2, Ti_3AlC_2 can resist KOH hot corrosion in 2 h. Ti_3AlC_2 suffered serious corrosion attack if the mass ratio⩾3. The main compositions of corroded samples were amorphous graphite and potassium titanates ($K_2O{\cdot}nTiO_2$). If the samples were washed by acid and dried, potassium titanates could decompose to K_2O and amorphous rutile. Based on the experimental results, a corrosion mechanism of Ti_3AlC_2 in molten KOH was proposed.

Keywords: Ti_3AlC_2; Raman spectroscopy; alkaline corrosion; hot corrosion

1 Introduction

Ti_3AlC_2 is a member of a group of ternary carbides and nitrides known as MAX phases with more than 70 members [1]. MAX phases are governed by the general formula $M_{n+1}AX_n$, where n = 1, 2 or 3, M is an early transition metal, A is an A-group element (mostly groups 13 and 14), and X is carbon and/or nitrogen [2]. MAX phases are layered hexagonal nano-laminated (space group $P6_3/mmc$) with two formula units per unit cell. In their crystal structure, near close-packed M layers are interleaved with layers of A elements with X filling the octahedral sites of M. Benefited from their unique structure, MAX phases combine both ceramic and metal performances and this makes them become a kind of promising materials applied in various areas.

Hot corrosion behavior is important for the application of MAX phases in hazardous environments. In recent decades, a significant number of literatures have reported the oxidation of MAX phases at high temperature [3–12]. For example, Ti_3AlC_2 has excellent oxidation resistance, which is attributed to the formation of two-layer dense and adherent passivating films. The inner is a continuous alpha-Al_2O_3 layer, while the outer is a rutile TiO_2 layer [3,5,10]. Hot corrosion of MAX phases in molten salts was also reported by literatures [13–16]. For instance, Cr_2AlC exhibits exceptionally good hot corrosion resistance against molten Na_2SO_4 salt due to the formation of a protective Al_2O_3-rich scale at 800–1300 ℃ in air [7]. It was reported that Ti_3SiC_2 suffers serious hot corrosion attack in the mixture of Na_2SO_4–NaCl melts if the concentration of Na_2SO_4 is higher than 35 wt% [14]. Additionally, if Ti_3SiC_2 is placed in molten cryolite [17] or molten Al [18], Si escapes and leaves the formation of TiC_x.

There also exist several papers on the corrosion of MAX phases in acids and dilute alkali [19–21]. According to the previous work, Ti_3AlC_2 displays good

* Corresponding author.
E-mail: zhouag@gmail.com; zhouag@hpu.edu.cn

corrosion resistance in 1 M NaOH solution owing to the formation of two-layer passivating films mainly consisting of titanium oxides. However, intergranular corrosion occurs while Ti_3AlC_2 immerses in 1 M H_2SO_4 solution. Xie *et al.* [22] investigated the selected MAX phases in a hot concentrated HCl solution. The reactivity of MAX phases strongly depends on the reactivity of A element (Al or Si) with the acid. Al-containing MAX phases suffer severe corrosion, whereas Si-containing Ti_3SiC_2 survives.

Based on the aforementioned research, Ti_3AlC_2 exhibits excellent corrosion resistance to alkali solution at room temperature. However, how is its corrosion resistance to alkali at high temperature? This is valuable for the application of Ti_3AlC_2 at high temperature in the condition with alkali. As far as we know, there is no literature related to this topic.

Accordingly, novel materials with unique structures and properties are made from acid etched products of Ti_3AlC_2. Naguib *et al*. [23,24] reported that 2D nano-sheets, composed of a few Ti_3C_2 layers and conical scrolls, were produced by removing Al element from Ti_3AlC_2 using hydrofluoric acid etching at room temperature. This discovery opens a door to the synthesis of a large number of 2D crystals. Even more, if both Al and Ti elements are removed from Ti_3AlC_2 by high-temperature chlorination, a porous carbon known as carbide-derived carbon is obtained, which is with unique pore structure and important applications [25,26].

Thus, novel materials with important application can be made by removing Al element using acid etching at room temperature or removing Al and Ti elements using Cl_2 etching at high temperature from Ti_3AlC_2. Can another novel material be made from alkali etching of Ti_3AlC_2 at high temperature? Since KOH etching is a normal method to make porous active carbon, it is interesting to research KOH-etching Ti_3AlC_2 at high temperature.

Therefore, in order to investigate the hot corrosion resistance to alkali and check whether a novel material can be made from the hot corrosion, this paper studied the corrosion response of Ti_3AlC_2 powders in molten KOH at 700 ℃.

2 Materials and experiment

Ti_3AlC_2 (−325 mesh, 98 wt% purity) was lab-made by tube furnace in Ar atmosphere from powder mixture of Ti, Al and C. KOH (85 wt% purity, K_2CO_3 as major impurity phase) was purchased from Tianjin Dalu Chemical Reagent Company, China. All corrosion experiments were done in a self-assembled nickel reactor. The reactor mainly consisted of a furnace body, a temperature control system and a nickel chamber. The temperature was controlled with a 10 ℃ deviation.

Mixed KOH–Ti_3AlC_2 powders were prepared according to KOH:Ti_3AlC_2 mass ratio of 1:1, 2:1, 3:1 and 4:1, respectively. In every experiment, mixture powders were placed in nickel crucible, gradually heated to 700 ℃ with a heating rate of 15 ℃/min, then kept at that temperature for 2 h, and finally removed from the reactor after the system cooled down to ambient temperature. Before each experiment, the nickel chamber was purged with high-purity N_2 for 15 min to minimize oxygen contamination. Since then, the system was bathed in a stream of N_2, until the reactions were finished and samples were removed from the reactor. The final products were evenly divided into two groups: one was directly washed by deionized water (marked with group A), while the other was immersed in 1 mol/L HCl solution (marked with group B) for 15 min and then washed by deionized water. The groups were both washed repeatedly until the pH value of residual solution reached 6–7 (samples numbered in Table 1). Thereafter, all residual solid products were dried at 120 ℃ in an oven for 2 h, and subsequently ground in an agate mortar.

X-ray diffraction (XRD) patterns of the samples were obtained by a powder diffractometer (Brook AXS, German) with Cu Kα radiation and a step scan of 0.02°. Raman spectra of the samples were recorded by a Raman spectrometer (inVia, Renishawplc, Gloucestershire, UK) at room temperature using an Ar laser with wavelength of 514.5 nm as the excitation source. Microstructure of the samples was observed by a 6301F field emission scanning electron microscope

Table 1 List of samples and corrosion products

Mass ratio of KOH:Ti_3AlC_2	1:1	2:1	3:1	4:1
Sample	1	2	3	4
Washed by deionized water/group A	A1	A2	A3	A4
Immersed in HCl solution/ group B	B1	B2	B3	B4

(SEM, JSM-6390LV, JEOL, Japan) equipped with an energy dispersive spectroscopy system (EDS, INCA-ENERAGY 250, Oxford, UK).

3 Results and discussion

The XRD patterns of group A and group B are almost the same, thus here we only show the XRD patterns of group A in Fig. 1.

From Fig. 1, all characteristic peaks of Ti_3AlC_2 decrease and finally vanish as the mass of KOH increases. If KOH:Ti_3AlC_2 = 1 or 2, the sharp peaks of Ti_3AlC_2 are still obvious and no peak of other phases appears. Therefore, Ti_3AlC_2 can resist the corrosion attack of KOH at 700 ℃ within 2 h if KOH: $Ti_3AlC_2 \leqslant 2$. If the mass ratio reaches to 3 or 4 (the top two patterns of Fig. 1), no sharp peak of crystalline phases exists except for a weak broaden peak at ~28°. Additionally, selected area electron diffraction (SAED) of those samples (not shown) only show diffuse rings. Therefore, if KOH:Ti_3AlC_2 = 3 or 4, Ti_3AlC_2 is completely consumed and the main phase of corroded products is amorphous.

To know more about the amorphous corroded phases, they were investigated by Raman spectroscopy. Firstly, a large amount of amorphous graphite exists in the corroded phase, which is strongly demonstrated by the peaks located at ~1348 cm^{-1} and ~1580 cm^{-1} appearing in Raman spectra of all the corroded samples (not shown). Besides amorphous graphite, there are potassium titanates ($K_2Ti_6O_{13}$) [27] and rutile (TiO_2) detected in group A and group B as shown in Fig. 2 and Fig. 3, respectively. In both figures, the peaks are gradually left-shifted and sharpened as KOH ratio increases. According to the Raman spectra in the literature [27], the sharp peaks labeled with numbers in Fig. 2 belong to $K_2Ti_6O_{13}$, which is sensitive to Raman spectroscopy [28,29]. However, the corresponding peaks in Fig. 3 are attributed to rutile (TiO_2) at the same condition. Agreed with the Raman result, potassium atoms are detected by EDS in the samples of group B.

Among several types of potassium titantates, $K_2Ti_6O_{13}$ is relative stable and easily hydrolyzed to amorphous TiO_2 [27]. Therefore, it is reasonable to conclude that amorphous $K_2Ti_6O_{13}$ transforms to amorphous TiO_2 in the acid solution by the following reactions:

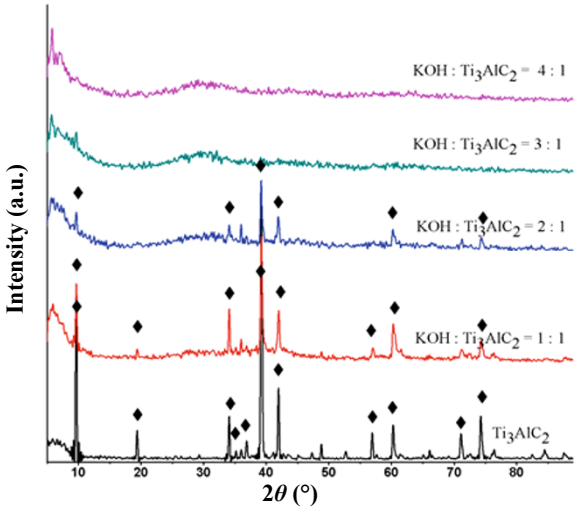

Fig. 1 XRD patterns of group A and Ti_3AlC_2.

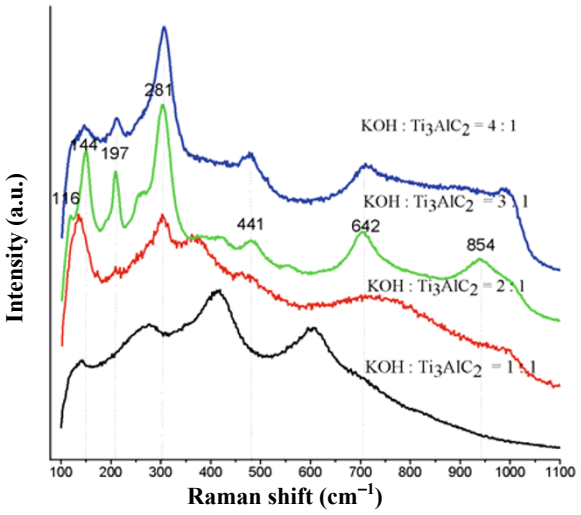

Fig. 2 Raman spectra of group A.

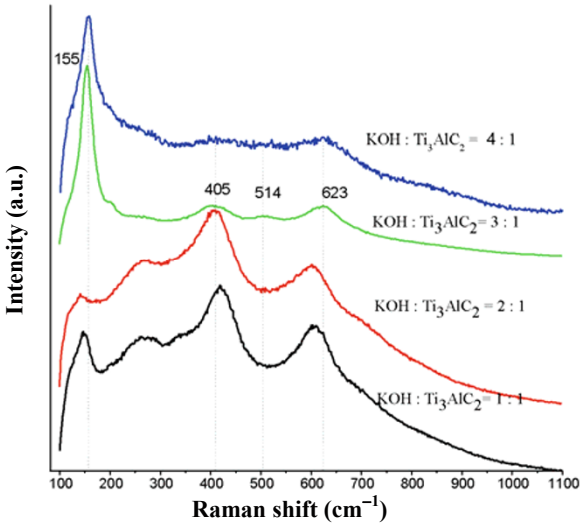

Fig. 3 Raman spectra of group B.

$$K_2Ti_6O_{13}(s)+2H^+ \longrightarrow 2H^+ +H_2Ti_6O_{13}(s) \quad (1)$$

$$H_2Ti_6O_{13}(s) \xrightarrow{120℃} 6TiO_2(s)+H_2O(g) \quad (2)$$

where s and g denote the state of solid and gas, respectively. The presence of H^+ due to acid washing promotes Reaction 1 and finally results that all $K_2Ti_6O_{13}$ is converted to $H_2Ti_6O_{13}$. Thereafter, $H_2Ti_6O_{13}$ continuously decomposes to TiO_2 and water vapor when dried in an oven. Recently, layered $H_2Ti_6O_{13}$ nanowires have been fabricated by using potassium titanates as precursor, which are prepared through a facile hydrothermal method, and followed with an acid treatment and finally dried at 70 ℃ for 12 h [30]. This experiment process is similar to our work. However, $H_2Ti_6O_{13}$ produced in our experiment decomposes to TiO_2 because the temperature (120 ℃) for drying is probably too high.

A typical SEM image of group A2 is shown in Fig. 4 to reveal the microstructure of corroded product. Many micro-pores are observed on the sample's surface. In addition, some pores cluster and form cracks and holes, which eventually destroy the structure of layered Ti_3AlC_2. From the figure, a nano-laminar phase is noted, which is marked with a red rectangle. EDS analysis demonstrates that the elements in this region contain Ti, O, K, C and a small amount of Si. Interestingly, K:Ti ratio is approximately 2 in this case. From the results of EDS and Raman, this nano-laminar phase is most probably $K_2Ti_4O_9$.

Therefore, here we put forward a possible corrosion reaction:

$$yTi_3AlC_2(s)+(3x+y)KOH(s) \xrightarrow{700℃} 1.5xK_2O\cdot 3yTiO_{(z-0.5x)/y}(s)+yKAlO_2(s) +(3z+2y)H_2O(g)+2yC(s) \quad (3)$$

where s still stands for the state of solid, and x, y and z are constants, and $0.83 \leqslant x/y \leqslant 3.166$. At this reaction, due to amorphous state, the true values of x, y and z are unknown at this moment. However, it is true that as the mass of KOH increases, the value of $3y/1.5x$ increases but is limited between 2 and 3; therefore, $K_2Ti_4O_9$ and $K_2Ti_6O_{13}$ are detected in group A2, A3 and A4, respectively.

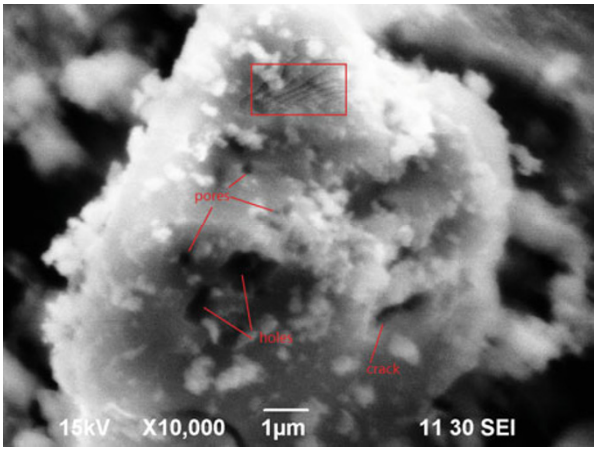

Fig. 4 SEM of group A2.

4 Conclusions

Ti_3AlC_2 can resist the corrosion of KOH at 700 ℃ if the mass ratio of KOH:Ti_3AlC_2 = 1 or 2. However, Ti_3AlC_2 suffers heavily hot corrosion attack if the mass ratio of KOH:$Ti_3AlC_2 \geqslant 3$. XRD and Raman spectroscopic results indicate that the corrosion products of Ti_3AlC_2 in molten KOH are mainly amorphous graphite and potassium titanates ($K_2O\cdot nTiO_2$), where $2 \leqslant n \leqslant 3$. As the mass of KOH increases, the value of n increases. The later would decompose to amorphous TiO_2 and K_2O if immersed in acid solution. SEM result demonstrates that corrosion morphologies involve pores, holes and cracks. Furthermore, nano-laminer $K_2Ti_4O_9$ is produced at appropriate conditions but its amount is quite little. Different from alkaline solution corrosion, no protective layers are found or detected. Further research is needed to investigate the whole corrosion mechanism.

Acknowledgements

This work was supported by the National Nature Science Foundation of China (Grant Nos. 51002045, 51205111), Program for Innovative Research Team of Henan Polytechnic University (T2013-4), and Opening Project of Henan Key Discipline Open Laboratory of Mining Engineering Materials (MEM12-5).

References

[1] Sun ZM. Progress in research and development on MAX phases: A family of layered ternary

compounds. *Int Mater Rev* 2011, **56**: 143–166.
[2] Barsoum MW. The $M_{N+1}AX_N$ phases: A new class of solids: Thermodynamically stable nanolaminates. *Prog Solid State Ch* 2000, **28**: 201–281.
[3] Gupta S, Filimonov D, Palanisamy T, *et al*. Tribological behavior of select MAX phases against Al_2O_3 at elevated temperatures. *Wear* 2008, **265**: 560–565.
[4] He LF, Lin ZJ, Bao YW, *et al*. Isothermal oxidation of bulk $Zr_2Al_3C_4$ at 500 to 1000 ℃ in air. *J Mater Res* 2008, **23**: 359–366.
[5] Li Z, Gao W, Zhang DL, *et al*. Oxidation behavior of a TiAl–$Al_2Ti_4C_2$–TiC–Al_2O_3 *in situ* composite. *Oxid Met* 2004, **61**: 339–354.
[6] Lin ZJ, Li MS, Wang JY, *et al*. Influence of water vapor on the oxidation behavior of Ti_3AlC_2 and Ti_2AlC. *Scripta Mater* 2008, **58**: 29–32.
[7] Lin ZJ, Li MS, Wang JY, *et al*. High-temperature oxidation and hot corrosion of Cr_2AlC. *Acta Mater* 2007, **55**: 6182–6191.
[8] Sonestedt M, Frodelius J, Sundberg M, *et al*. Oxidation of Ti_2AlC bulk and spray deposited coatings. *Corros Sci* 2010, **52**: 3955–3961.
[9] Tian W, Wang P, Kan Y, *et al*. Oxidation behavior of Cr_2AlC ceramics at 1,100 and 1,250 ℃. *J Mater Sci* 2008, **43**: 2785–2791.
[10] Wang XH, Zhou YC. High-temperature oxidation behavior of Ti_2AlC in air. *Oxid Met* 2003, **59**: 303–320.
[11] Wang XH, Zhou YC. Intermediate-temperature oxidation behavior of Ti_2AlC in air. *J Mater Res* 2002, **17**: 2974–2981.
[12] Wang XH, Zhou YC. Oxidation behavior of Ti_3AlC_2 powders in flowing air. *J Mater Chem* 2002, **12**: 2781–2785.
[13] Lin Z, Zhou Y, Li M, *et al*. Improving the Na_2SO_4-induced corrosion resistance of Ti_3AlC_2 by pre-oxidation in air. *Corros Sci* 2006, **48**: 3271–3280.
[14] Liu G, Li M, Zhou Y, *et al*. Hot corrosion behavior of Ti_3SiC_2 in the mixture of Na_2SO_4–NaCl melts. *J Eur Ceram Soc* 2005, **25**: 1033–1039.
[15] Wang XH, Zhou YC. Hot corrosion of Na_2SO_4-coated Ti_3AlC_2 in air at 700–1000 ℃. *J Electrochem Soc* 2004, **151**: B505–B511.
[16] Lin Z, Zhou Y, Li M, *et al*. Hot corrosion and protection of Ti_2AlC against Na_2SO_4 salt in air. *J Eur Ceram Soc* 2006, **26**: 3871–3879.
[17] Barsoum MW, El-Raghy T, Farber L, *et al*. The topotactic transformation of Ti_3SiC_2 into a partially ordered cubic $Ti(C_{0.67}Si_{0.06})$ phase by the diffusion of Si into molten cryolite. *J Electrochem Soc* 1999, **146**: 3919–3923.
[18] El-Raghy T, Barsoum MW, Sika M. Reaction of Al with Ti_3SiC_2 in the 800–1000 ℃ temperature range. *Mat Sci Eng A* 2001, **298**: 174–178.
[19] Li D, Liang Y, Liu X, *et al*. Corrosion behavior of Ti_3AlC_2 in NaOH and H_2SO_4. *J Eur Ceram Soc* 2010, **30**: 3327–3234.
[20] Travaglini J, Barsoum MW, Jovic V, *et al*. The corrosion behavior of Ti_3SiC_2 in common acids and dilute NaOH. *Corros Sci* 2003, **45**: 1313–1327.
[21] Jovic VD, Jovic BM, Gupta S, *et al*. Corrosion behavior of select MAX phases in NaOH, HCl and H_2SO_4. *Corros Sci* 2006, **48**: 4274–4282.
[22] Xie J, Wang X, Li A, *et al*. Corrosion behavior of selected $M_{n+1}AX_n$ phases in hot concentrated HCl solution: Effect of A element and MX layer. *Corros Sci* 2012, **60**: 129–135.
[23] Naguib M, Kurtoglu M, Presser V, *et al*. Two-dimensional nanocrystals produced by exfoliation of Ti_3AlC_2. *Adv Mater* 2011, **23**: 4248–4253.
[24] Naguib M, Mashtalir O, Carle J, *et al*. Two-dimensional transition metal carbides. *ACS Nano* 2012, **6**: 1322–1331.
[25] Hoffman EN, Yushin G, Barsoum MW, *et al*. Synthesis of carbide-derived carbon by chlorination of Ti_2AlC. *Chem Mater* 2005, **17**: 2317–2322.
[26] Hoffman EN, Yushin G, El-Raghy T, *et al*. Micro and mesoporosity of carbon derived from ternary and binary metal carbides. *Microporous Mesoporous Mater* 2008, **112**: 526–532.
[27] Bamberger CE, Begun GM, MacDougall CS. Raman spectroscopy of potassium titanates: Their synthesis, hydrolytic reactions, and thermal stability. *Appl Spectrosc* 1990, **44**: 30–37.
[28] Bamberger CE, Begun GM. Sodium titanates: Stoichiometry and Raman spectra. *J Am Ceram Soc* 1987, **70**: C-48–C-51.
[29] Bamberger CE, Dunn HW, Begun GM, *et al*. Substitutional solid solutions of bismuth-containing lanthanide dititanates, $Ln_{2-x}Bi_xTi_2O_7$. *J Solid State Chem* 1985, **58**: 114–118.
[30] Wang Y, Hong Z, Wei M, *et al*. Layered $H_2Ti_6O_{13}$-nanowires: A new promising pseudocapacitive material in non-aqueous electrolyte. *Adv Funct Mater* 2012, **22**: 5185–5193.